DEVELOPMENTAL NEUROSCIENCE

Maternal diabetes induces senescence and neural tube defects sensitive to the senomorphic rapamycin

Cheng Xu[1], Wei-Bin Shen[1], E. Albert Reece[1,2], Hidetoshi Hasuwa[3†], Christopher Harman[1], Sunjay Kaushal[4], Peixin Yang[1,2*]

Neural tube defects (NTDs) are the second most common structural birth defect. Senescence, a state of permanent cell cycle arrest, occurs only after neural tube closure. Maternal diabetes–induced NTDs are severe diabetic complications that lead to infant mortality or lifelong morbidity and may be linked to premature senescence. Here, we report that premature senescence occurs in the mouse neuroepithelium and disrupts neurulation, leading to NTDs in diabetic pregnancy. Premature senescence and NTDs were abolished by knockout of the transcription factor *Foxo3a*, the *miR-200c* gene, and the cell cycle inhibitors *p21* and *p27*; transgenic expression of the dominant-negative FoxO3a mutant; or the senomorphic rapamycin. Double transgenic expression of p21 and p27 mimicked maternal diabetes in inducing premature neuroepithelium senescence and NTDs. These findings integrate transcription- and epigenome-regulated miRNAs and cell cycle regulators in premature neuroepithelium senescence and provide a mechanistic basis for targeting premature senescence and NTDs using senomorphics.

INTRODUCTION

Neural tube defects (NTDs), the second most common structural birth defect, greatly contribute to infant and lifelong mortality. Folate is the only method of NTD prevention but only prevents up to 70% of NTDs (*1*). NTDs are still highly prevalent. Globally, there are 300,000 to 400,000 cases per year, resulting in approximately 88,000 deaths and 8.6 million disability-adjusted life years. Annual medical and surgical costs for children born with NTDs in the United States are more than $200 million. Thus, new therapeutic targets need to be revealed for the development of new NTD prevention methods. Most human NTDs are caused by nongenetic factors. Maternal diabetes is a major and ever-rising nongenetic factor that induces NTDs (*2*). There are approximately 3 million Americans and 60 million women of reproductive age (15 to 44 years) worldwide with pregestational diabetes, making it urgent to discover the cause of diabetic embryopathy.

Using rodent models of diabetic embryopathy, our previous studies have demonstrated that maternal diabetes specifically induces NTDs by altering kinase activation and gene expression (*3*–*10*). However, how the molecular events downstream of hyperglycemia integrate and lead to failed neurulation are unknown. Neurulation, one of the critical and fundamental morphogenic processes of embryonic development, leads to central nervous system formation. Senescence in proliferating neuroepithelial cells may contribute to NTDs.

Cellular senescence in adult cells plays pleiotropic roles in many physiological and pathological processes, including aging, aging-related neurological disorders, tissue repair, tumorigenesis, and cardiovascular diseases. Recent studies have revealed that senescence also contributes to embryonic development (*11*, *12*). Developmental senescence, a newly found, normal programming mechanism, promotes tissue remodeling and directs embryonic development (*11*, *12*). Cellular senescence and developmental senescence share common characteristics, including senescence-associated β-galactosidase (SAβG) activity, heterochromatic foci, and acquisition of a senescence-associated secretory phenotype (SASP) (*11*–*13*). However, developmental senescence is unique from cellular senescence because it does not depend on the activation of the cellular DNA damage response or the p16 tumor suppressor pathway and does not produce some of the SASP factors (*11*, *12*). Developmental senescence is mediated by p21 and regulated by the Forkhead transcription factor (FoxO) and transforming growth factor–β/Smad pathways (*11*, *12*).

Developmental senescence occurs after neural tube closure on embryonic day 11 (E11) in the mouse (*11*, *12*). Cellular senescence inducers, including DNA damage and p53 up-regulation, have been observed in diabetic embryopathy (*14*, *15*). Strong evidence also suggests that apoptosis signal–regulating kinase 1 (ASK1), a mediator of cellular senescence induced by high glucose in vitro (*16*), plays a causal role in diabetes-induced NTDs (*8*). Last, maternal diabetes–induced oxidative stress triggers the activation and increase in the cellular senescence mediators ASK1, FoxO3a, and p53. Because antioxidants delay or prevent cellular senescence (*17*), oxidative stress may induce senescence. This evidence collectively implies that premature senescence in the developing neuroepithelium may be associated with diabetes-induced NTDs. The developing neuroepithelium is a highly proliferative and dynamic tissue (*18*). Neuroepithelial cells proliferate (*18*) to achieve a critical mass for the paired dorsolateral hinge points, which are critical for the two opposite neural folds to be contacted and fused (*18*). Altered neuroepithelial cell proliferation and differentiation and enhanced apoptosis are contributing factors in NTD pathogenesis (*8*, *9*, *19*). Thus, it is plausible that premature senescence in proliferative neuroepithelial cells would lead to failed neural tube closure in diabetic embryopathy.

The present study reveals that maternal diabetes triggers premature developmental senescence (hereafter referred to as premature senescence) in neuroepithelial cells during neurulation, thereby leading to NTD formation. The FoxO3a-miR200c pathway silenced

[1]Department of Obstetrics, Gynecology and Reproductive Sciences, University of Maryland School of Medicine, Baltimore, MD, USA. [2]Department of Biochemistry and Molecular Biology, University of Maryland School of Medicine, Baltimore, MD, USA. [3]Department of Molecular Biology, Keio University School of Medicine, 35 Shinanomachi Shinjuku-ku, Tokyo 160-8582, Japan. [4]Department of Surgery, University of Maryland School of Medicine, Baltimore, MD, USA.
*Corresponding author. Email: pyang@som.umaryland.edu
†Present address: Laboratory Animal Center, Keio University School of Medicine, Tokyo 160-8582, Japan.

the transcriptional repressor zinc finger E-box binding homeobox 1/2 (ZEB1/2), leading to up-regulation of the senescence mediators p21 and p27. Overexpression of p21 and p27 in the developing neuroepithelium mimicked diabetes in inducing neuroepithelial cell senescence and NTDs. Since senomorphics and senolytics, which inhibit the ontogeny of senescence and selectively remove senescent cells, respectively, are proposed as a new generation of human disease therapeutics (*20*, *21*), we determined the therapeutic effect of the senomorphic rapamycin on diabetes-induced NTDs. Thus, premature senescence in the developing neuroepithelium is critically involved in NTD formation in diabetic pregnancy, and rapamycin may be an effective therapeutic.

RESULTS

Maternal diabetes induces premature senescence in the neuroepithelium

We found that mice with maternal diabetes exhibited a robust staining signal of SAβG, a well-recognized senescence marker, in the anterior neuroepithelium on E8.5 (Fig. 1A), suggesting that senescence targets a population of proliferative cells in the neuroepithelium (*18*, *22*, *23*). The induction of the major developmental senescence mediator p21 (*11*, *12*) was observed at E8.0 in the same region (Fig. 1B), preceding the SAβG signal at E8.5 onward (Fig. 1A), suggesting that p21 may trigger senescence in diabetic embryopathy. Cross-sectional analyses of the whole embryo revealed that the

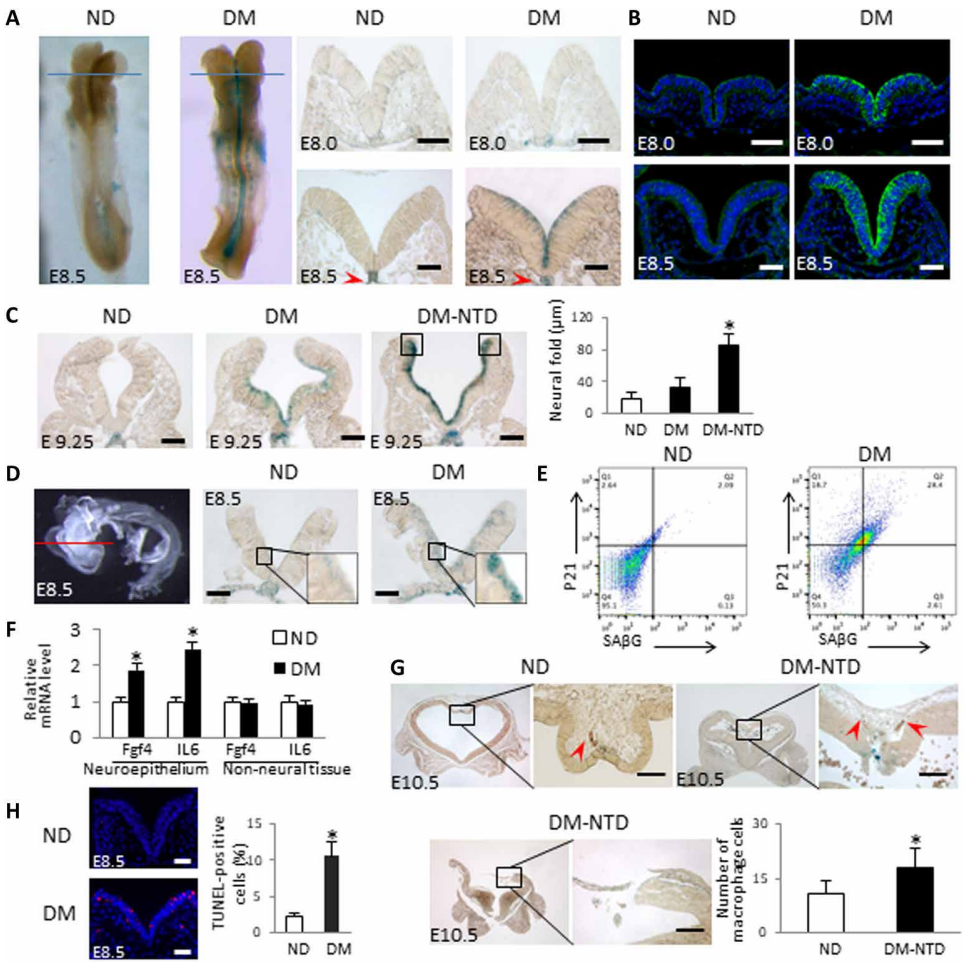

Fig. 1. Maternal diabetes induces premature senescence in the developing neuroepithelium. (**A**) Whole-mount staining of SAβG in E8.5 embryos (five to seven somite pairs) and coronal sections of E8.0 (two to four somites) and E8.5 embryos after SAβG staining. Blue line indicates the levels of sectioning. (**B**) Anti-p21 antibody staining of E8.0 and E8.5 embryo sections. Red arrowheads indicate the notochords. (**C**) Sections of E9.25 embryos after SAβG staining and quantification of the distance between the two neural fold fusing edges (square frames). (**D**) Neuroepithelia were isolated from E8.5 embryos by Dispase II treatment for SAβG staining. Red line indicates section positions. (**E**) Fluorescence-activated cell sorting analysis by anti-SAβG and anti-p21 antibody staining in cells of isolated E8.75 (8 to 10 somites) neuroepithelia. (**F**) mRNA abundances of Fgf4 and interleukin-6 (IL-6) in isolated neuroepithelia and non-neural tissues of E8.5 embryos. (**G**) Sections of E10.5 embryos after SAβG staining. Infiltrated macrophages identified by immunostaining of the macrophage marker F4/80 are indicated by red arrowheads. The graph shows the number of macrophages ($n = 3$). (**H**) Representative images of the terminal deoxynucleotidyl transferase–mediated deoxyuridine triphosphate nick end labeling (TUNEL) assays in E8.5 embryos and quantification of apoptotic cells. Apoptotic cells are labeled in red. Scale bars, 70 μm in (A) to (D) and (H) and 45 μm in (G). Embryos from three litters ($n = 3$) each group were analyzed. Two to three embryos from each litter and four to five sections per embryo were stained, and an average for signal intensity was obtained for that litter. ND, nondiabetic dams; DM, diabetic mellitus dams. Asterisk indicates a significant difference ($P < 0.05$) compared to other groups.

SAβG signal was induced by maternal diabetes in the anterior but not in the posterior neuroepithelium (fig. S1) and that the notochord was SAβG$^+$ under both nondiabetic and diabetic conditions (Fig. 1A and fig. S1). On E9.25, an intense SAβG signal was observed in the fusing tips of the two neural folds with a wide gap (Fig. 1C) and contributed to failed neural tube closure in diabetic pregnancy. At an early stage, the dorsal edges of neural folds did not contain senescent cells (Fig. 1A), suggesting that, at E9.25, cells at these sites become proliferative and are thus susceptible to senescence.

The SAβG signal was confirmed in isolated neuroepithelia that avoided the possible X-gal penetration problem during staining (Fig. 1D). Flow cytometry analysis was used to further characterize the features of senescent cells in the neuroepithelium. SAβG$^+$ cells were costained with p21 in isolated neuroepithelial cells (Fig. 1E): 92% of SAβG$^+$ cells were p21$^+$, and diabetes increased the number of double-stained SAβG$^+$ and p21$^+$ cells by approximately 14-fold (Fig. 1E). Senescent cells also exhibited the SASP, which adversely affects neighboring cells. The expression of two SASP factors, interleukin-6 and fibroblast growth factor 4, was significantly increased in the neuroepithelia of embryos exposed to diabetes (Fig. 1F). Senescent cells are removed by macrophages and induce apoptosis of neighboring cells. Increased macrophage infiltration in the SAβG$^+$ cell area was observed in the defective neuroepithelia of some NTD embryos (Fig. 1G), whereas other NTD embryos completely lost the SAβG$^+$ portions of their neuroepithelia (Fig. 1G). Apoptotic cells were mainly present on the SAβG$^+$ cells of the neuroepithelium (Fig. 1H). Thus, maternal diabetes induces premature senescence in the developing neuroepithelium, which resembles the key features of developmental senescence (*11*, *12*).

Deleting the *Foxo3a* gene diminishes premature senescence in diabetic pregnancy

FoxO3a, which is critically involved in developmental senescence (*12*), is activated and participates in maternal diabetes–induced NTDs (*8*). To determine whether FoxO3a is responsible for maternal diabetes–induced premature senescence in the developing neuroepithelium, three types of embryos were examined: wild type (WT), *Foxo3a* deleted, and FoxO3a dominant negative (DN-FoxO3a). *Foxo3a* deletion diminished the signals of SAβG, the DNA damage marker γH2AX, and the heterochromatin marker histone H3 trimethylation at lysine-9 (H3K9me3) (Fig. 2, A and B). It also restored phospho-histone H3 (p-H3) signals, which showed

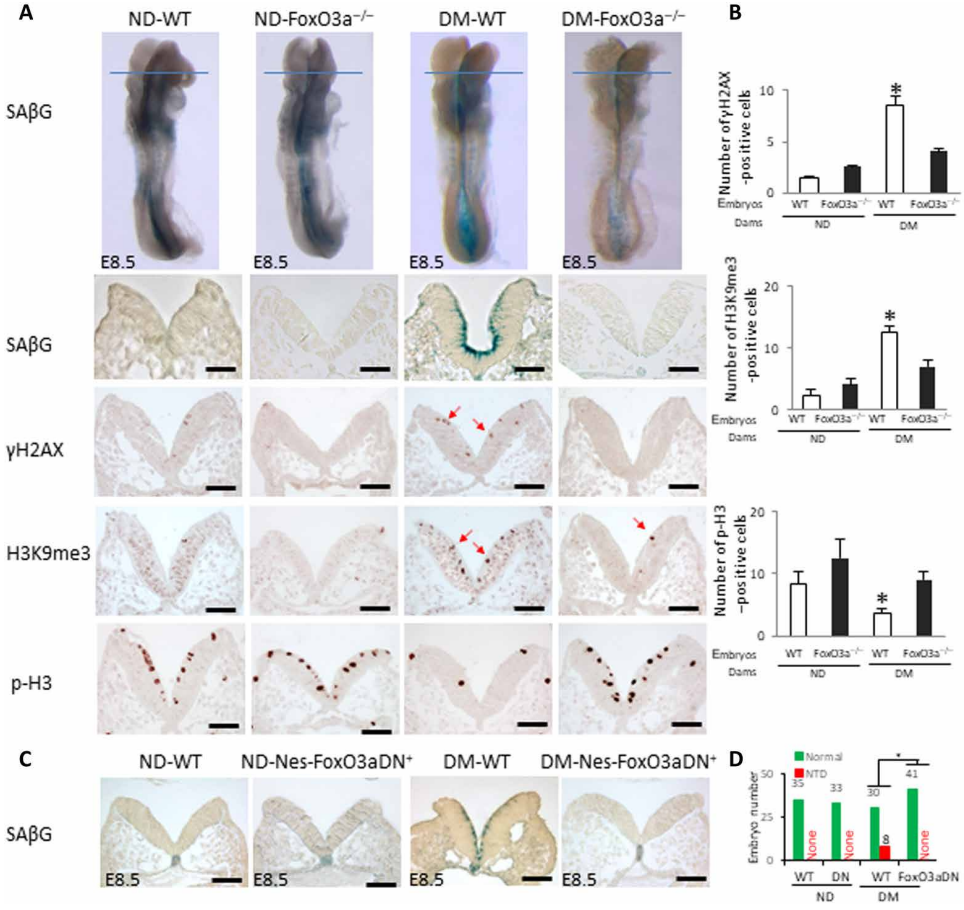

Fig. 2. FoxO3a is essential for maternal diabetes–induced premature senescence. (**A**) SAβG staining and anti-γH2AX, anti-H3K9me3, and anti–p-H3 antibody staining. Blue lines indicate the levels of sectioning shown below. Quantification of antibody staining–positive cells is shown in (**B**). (**C**) Sections of SAβG staining on E8.5 (five to seven somites) WT and Nestin-Foxo3a-DN embryos. (**D**) NTD rates of WT and Nestin-FoxO3a-DN embryos. Green bars, normal embryos; red bars, NTD embryos. Scale bars, 70 μm in (A) and (C). Embryos from three litters ($n = 3$) each group were analyzed. Two to three embryos from each litter and four to five sections per embryo were stained, and an average for signal intensity was obtained for that litter. Asterisk indicates a significant difference ($P < 0.05$) compared to other groups.

proliferating cells in metaphase in the E8.5 neuroepithelia exposed to maternal diabetes (Fig. 2, A and B). Diabetes-induced increases in abundances of p21 and p27 and DNA damage response proteins [p-checkpoint kinase 1 (p-CHK1), p-CHK2, γH2AX, and p53] were abrogated by *Foxo3a* deletion in whole embryos (fig. S2A).

DN-FoxO3a overexpression in embryos lacking the transactivation domain from the C terminus (*24*) had a similar effect as *Foxo3a* deletion on blocking maternal diabetes–induced premature senescence (Fig. 2C). In addition, DN-FoxO3a overexpression in the neuroepithelium ablated the increases in p21, p27, p-CHK1, and p-CHK2 protein in whole embryos (fig. S2B). Consistent with previous findings that *Foxo3a* deletion significantly reduces NTDs in diabetic pregnancy (*8*), embryos overexpressing DN-FoxO3a had a significantly lower NTD incidence than their WT littermates from diabetic dams (Fig. 2D and table S1). Because DN-FoxO3a lacks transcriptional activity (*24*), the above observations implicate a transcriptional mechanism underlying FoxO3a-mediated premature senescence in diabetic embryopathy.

Maternal diabetes–activated FoxO3a induces miR-200c expression

MicroRNAs (miRNAs) are small endogenous noncoding RNAs that suppress gene expression at the posttranscriptional level (*25*), and they play important roles in embryonic development (*26*). Recent evidence shows the critical involvement of miRNAs in mouse neurulation (*27*), NTDs in human pregnancies (*28*), and mechanisms underlying diabetic embryopathy (*7*, *29*). miRNAs have been identified as novel inducers of cellular senescence (*30*–*32*). We hypothesized that a miRNA mediates premature senescence in diabetic embryopathy. We focused on miR-200c because it is involved in inducing senescence in cell culture systems (*31*). Two FoxO3a binding sites were found in the promoter region of the miR-200 cluster (Fig. 3A). Constitutively active (CA) FoxO3a mimicked high-glucose–induced miR-200 promoter activity in cultured neural stem cells (Fig. 3A), whereas DN-FoxO3a blocked the stimulatory effect of high glucose on miR-200 transcription (Fig. 3A). Either *Foxo3a* deletion or DN-FoxO3a overexpression in the developing neuroepithelium abolished the increase in miR-200c in embryos of diabetic pregnancies (Fig. 3B and fig. S3).

miR-200c mediates the effect of maternal diabetes on the induction of senescence and NTDs

To investigate whether miR-200c plays a role in maternal diabetes–induced neuroepithelial senescence and NTD formation, heterozygous *miR-200c* knockout (KO) mice were used to generate WT, *miR-200c* heterozygous, and null embryos under the same maternal conditions (table S2). *miR-200c* heterozygous embryos had an insignificant reduction in NTDs, whereas *miR-200c*-null embryos had a significantly lower NTD incidence than WT embryos from diabetic dams (Fig. 3C and table S2). The NTD incidence in *miR-200c*-null embryos was significantly lower than that in *miR-200c* heterozygous embryos under diabetic conditions (Fig. 3C and table S2). miR-141 is the closest member of miR-200c in the miR-200 family (*33*). *miR-141* was also deleted in the miR-200c KO mice (fig. S4). To ascertain whether miR-200c is critical for the NTD reduction in miR-200c-null embryos, we generated *miR-200c*$^{-/-}$ embryos with miR-141 transgene expression in the neuroepithelium (table S3). Restoring miR-141 expression did not alter the inhibitory effect of *miR-200c* deletion on maternal diabetes–induced NTDs (table S3). miR-200c overexpression in the neuroepithelium did not induce NTDs (table S4), suggesting that other miRNAs, possibly miR-200b (*7*), co-mediate the teratogenicity of maternal diabetes with miR-200c and that miR-200c itself cannot reach the threshold leading to NTD formation. However, miR-200c overexpression neutralized the beneficial effect of *miR-200c* deletion on reducing diabetes-induced NTDs (table S4), supporting the specificity of miR-200c deletion in NTD reduction.

To elucidate the mechanism underlying *miR-200c* deletion–reduced NTDs, indices of premature senescence in the neuroepithelium were analyzed. Maternal diabetes–induced increases in p21, p27, p-CHK1, and p-CHK2 in whole embryos were significantly attenuated by miR-200c deletion (Fig. 3, D and E). *miR-200c* deletion significantly decreased the signals of SAβG, γH2AX, p53, and H3K9me3 and restored the cell proliferation marker p-H3 signal in the anterior neuroepithelium (Fig. 4, A to D). These results suggest that miR-200c is responsible for the up-regulation of the senescence inducer–induced DNA damage signaling.

miR-200c silences the transcriptional repressors ZEB1 and ZEB2

To search for the direct targets of miR-200c, we focused on ZEB1 and ZEB2, two transcriptional repressors of the senescence mediator p21 (*31*, *34*). An online miR target prediction algorithm (miRanda) revealed several binding sites of miR-200c in ZEB1 and ZEB2 mRNAs (fig. S5A). To determine whether miR-200c targets ZEB1 and ZEB2 mRNA, we performed an RNA pull-down assay using biotin-labeled miR-200c in cultured neural stem cells. Cells transfected with biotin-labeled miR-200c had a high level of miR-200c (fig. S5B). ZEB1 and ZEB2 mRNAs were enriched approximately sixfold in biotin-labeled miR-200c (fig. S5B). The miR-200c inhibitor increased ZEB1 and ZEB2 expression under normal-glucose conditions and rescued ZEB1 and ZEB2 expression under high-glucose conditions (Fig. 3F). The miR-200c mimic significantly decreased ZEB1 and ZEB2 expression under normal-glucose conditions (Fig. 3G) and thus simulated the effect of high glucose on ZEB1 and ZEB2 repression. Therefore, miR-200c represses ZEB1 and ZEB2 expression by degrading mRNA and inhibiting translation. Consistent with the up-regulation of miR-200c, ZEB1 and ZEB2 protein abundance in whole embryos was significantly reduced by maternal diabetes (Fig. 4E). *miR-200c* deletion abrogated maternal diabetes–induced ZEB1 and ZEB2 down-regulation (Fig. 4E). These findings support the hypothesis that miR-200c induces premature senescence by removing the p21 and p27 promoter repressors ZEB1 and ZEB2 (*35*, *36*).

p21 and p27 are premature senescence mediators in diabetic pregnancy

To investigate whether the FoxO3a–miR-200c–ZEB1/2 pathway converges on the senescence mediators p21 and p27, leading to failed neurulation, we used p21 KO and p27 KO mice (tables S5 and S6). *p21* heterozygous embryos displayed an insignificant reduction in NTDs, whereas *p21*-null embryos of diabetic dams had a significantly lower NTD incidence than WT embryos (Fig. 5A and table S5). To validate the specificity of *p21* deletion on NTD reduction, the p21 transgene was introduced to p21 KO mice (table S7). Restoring p21 expression in the neuroepithelium of *p21*-null embryos of diabetic dams abolished the NTD reduction (table S7). *p21* deletion reduced the SAβG, γH2AX, and H3K9me3 signals, and it restored staining of the cell proliferation marker p-H3 in the

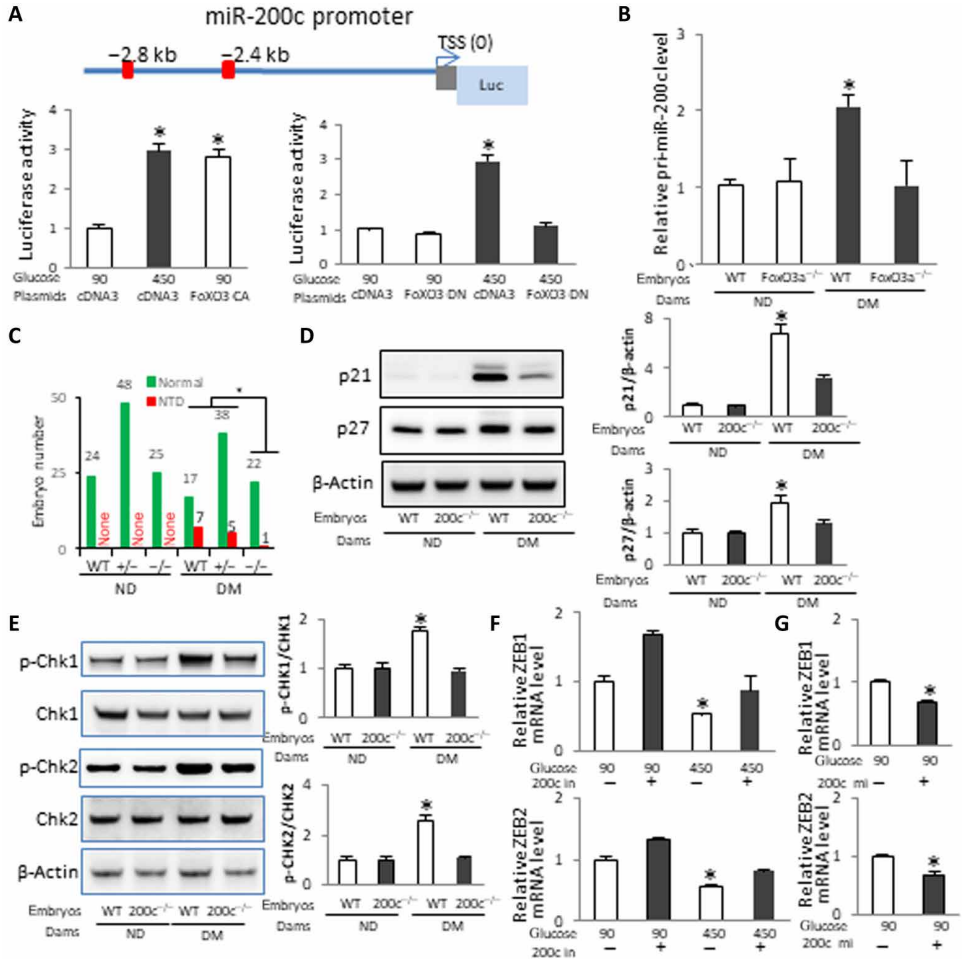

Fig. 3. miR-200c downstream of FoxO3a is critically involved in maternal diabetes–induced premature senescence and NTDs. (**A**) Schematic of the miR-200 promoter-luciferase construct. A 3.6-kb genomic fragment from the miR-200 promoter region was cloned into the pGL4.10 vector. Red squares indicate FoxO3a binding sites. The relative luciferase activity (Luc) in cultured neural stem cells after cotransfection with a blank vector control, FoxO3a CA, and DN expression vectors is shown. The experiment was run in triplicate. (**B**) pri-miR-200c abundance in WT and FoxO3a mutant embryos in E8.5 (five to seven somites). Embryos from three litters ($n = 3$) each group and two to three embryos from each litter were analyzed. (**C**) NTD rates of WT, miR-200c-null, and heterozygous E10.5 embryos. Green bars, normal embryos; red bars, NTD embryos. Protein abundance of p21 and p27 (**D**) and phosphorylated Chk1 (p-Chk1), Chk1, p-Chk2, and Chk2 (**E**) in E8.5 embryos from three litters each group. Bar graphs of protein abundance are quantitative data from three independent experiments. The mRNA abundances of ZEB1 and ZEB2 were affected by the miR-200c inhibitor (**F**) and the miR-200c mimic (**G**) in neural stem cells ($n = 3$). TSS, transcription starting site. Asterisk indicates a significant difference ($P < 0.05$) compared to other groups.

anterior neuroepithelium induced by maternal diabetes (Fig. 5, B and C). The induction of the DNA damage markers p-CHK1, p-CHK2, γH2AX, and p53 in whole embryos by maternal diabetes was suppressed by *p21* deletion (Fig. 5, D and E), suggesting that the DNA damage response is a downstream event of p21-induced senescence. ZEB1 and ZEB2 down-regulation and miR-200c up-regulation in whole embryos were unaffected by *p21* deletion (Fig. 5, F and G), indicating that they are upstream of p21 in the premature senescence pathway.

p27 deletion had a similar effect as *p21* deletion, leading to a significant reduction in NTDs in diabetic pregnancies (Fig. 6A and table S6), and heterozygous *p27* deletion slightly reduced NTD formation (Fig. 6A and table S6). *p27* deletion effectively suppressed maternal diabetes–induced premature senescence by blocking the SAβG, γH2AX, and H3K9me3 signals and restoring cell proliferation in neurulation-stage embryos (Fig. 6, B and C). Because either *p21* or *p27* deletion significantly reduced NTDs, the additive effect of double deletion was not expected and was thus not assessed.

Double overexpression of p21 and p27 in the neuroepithelium mimics diabetes-induced NTDs

The critical involvement of both p21 and p27 in maternal diabetes–induced premature neuroepithelium senescence leading to NTD formation was exemplified by the fact that embryos with *p21* and *p27* double transgene expression in the developing neuroepithelium had a similar NTD incidence as those from diabetic pregnancies (Fig. 7, A and B, and table S8). Premature senescence was manifested in the anterior neuroepithelia in *p21* and *p27* double-overexpressing embryos (Fig. 7, C and D).

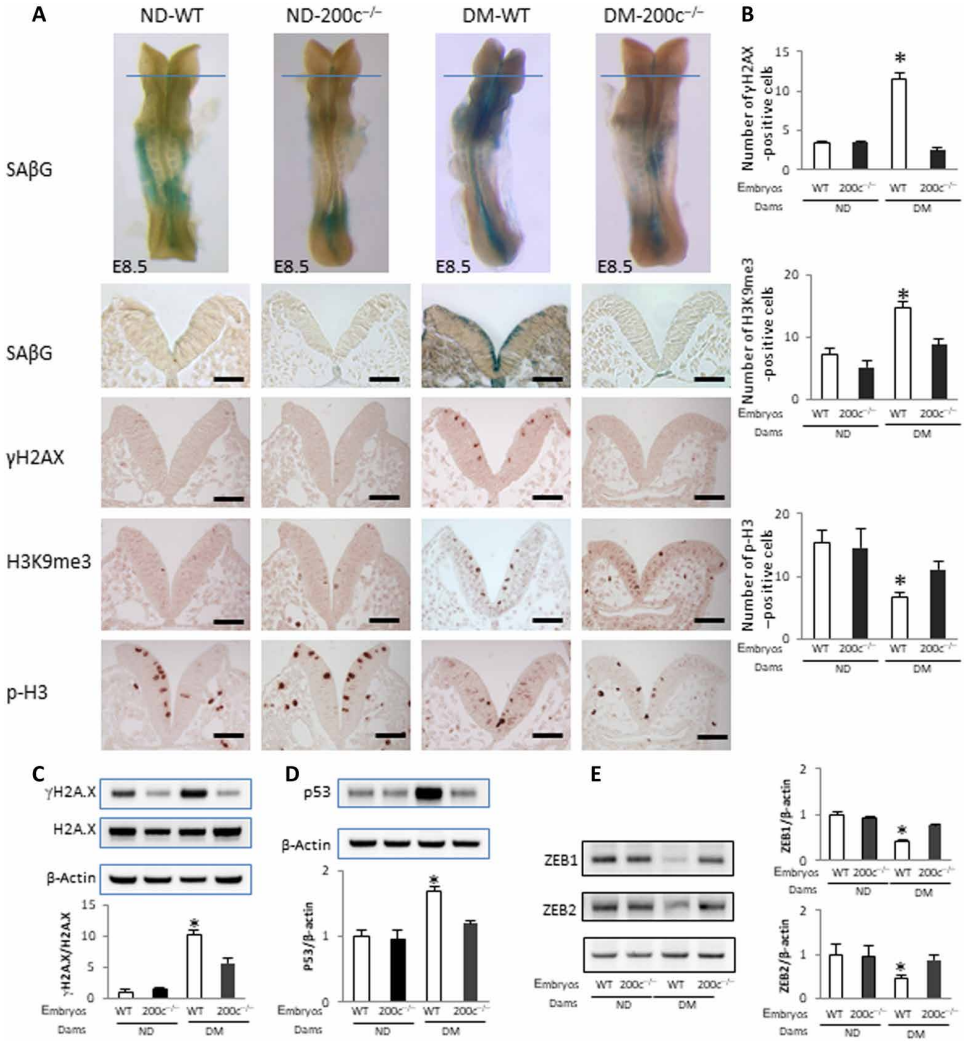

Fig. 4. miR-200c mediates maternal diabetes–induced premature senescence. (**A**) SAβG staining and antibody staining for γH2AX, H3K9me3, and p-H3. Quantification of antibody staining–positive cells is shown in (**B**). Protein abundance of γH2AX, H2AX (**C**), p53 (**D**), and ZEB1 and ZEB2 (**E**) in E8.5 (five to seven somites) embryos. Bar graphs for protein abundance are quantitative data from three independent experiments ($n = 3$). Scale bars, 70 μm. Asterisk indicates a significant difference ($P < 0.05$) compared to other groups.

Rapamycin inhibits premature senescence and reduces NTD formation

It has been shown that the mechanistic target of rapamycin (mTOR) inhibitor rapamycin acts as a senomorphic agent to suppress cellular senescence (*37*). To investigate whether rapamycin inhibits maternal diabetes–induced premature senescence in the developing neuroepithelium, pregnant WT diabetic and nondiabetic control mice received rapamycin via intraperitoneal injections at a daily dose of 2 mg/kg of body weight from E5.5 to E8.5 or E10.5.

Embryos from diabetic dams treated with rapamycin had a significantly lower NTD incidence than embryos from diabetic dams without rapamycin treatment (Fig. 8, A and B, and table S9). Rapamycin could be readily detected in the embryos of dams that received treatment (table S9). Rapamycin treatment diminished maternal diabetes–induced signals of SAβG, γH2AX, and H3K9me3 and restored the cell proliferation marker p-H3 in the developing neuroepithelium of neurulation-stage embryos (Fig. 8, C and D). Rapamycin significantly reduced the number of apoptotic neuroepithelial cells induced by maternal diabetes (Fig. 8, C and D). Furthermore, rapamycin blocked the increase in the senescence mediator p21 and the activation of the DNA damage response proteins p-CHK1, p-CHK2, γH2AX, and p53 (Fig. 8, E to I) and reversed the repression of ZEB1 and ZEB2 (Fig. 8J) in whole embryos.

DISCUSSION

Senescence has just been recognized as a new mechanism for human adulthood diseases. Drugs that target senescent cells, known as senotherapeutics, work by inhibiting senescence initiation (senomorphic drugs) or by removing senescent cells (senolytic drugs) and have just been tested in small-scale clinical trials (*38*). In the current study, we revealed that premature senescence in the developing neuroepithelium contributes to the induction of NTDs caused by maternal diabetes in pregnancy. This form of premature senescence is initiated by transcriptional and epigenetic alterations of neurogenesis via the FoxO3a–miR-200c–ZEB1/2–p21/p27 pathway. On

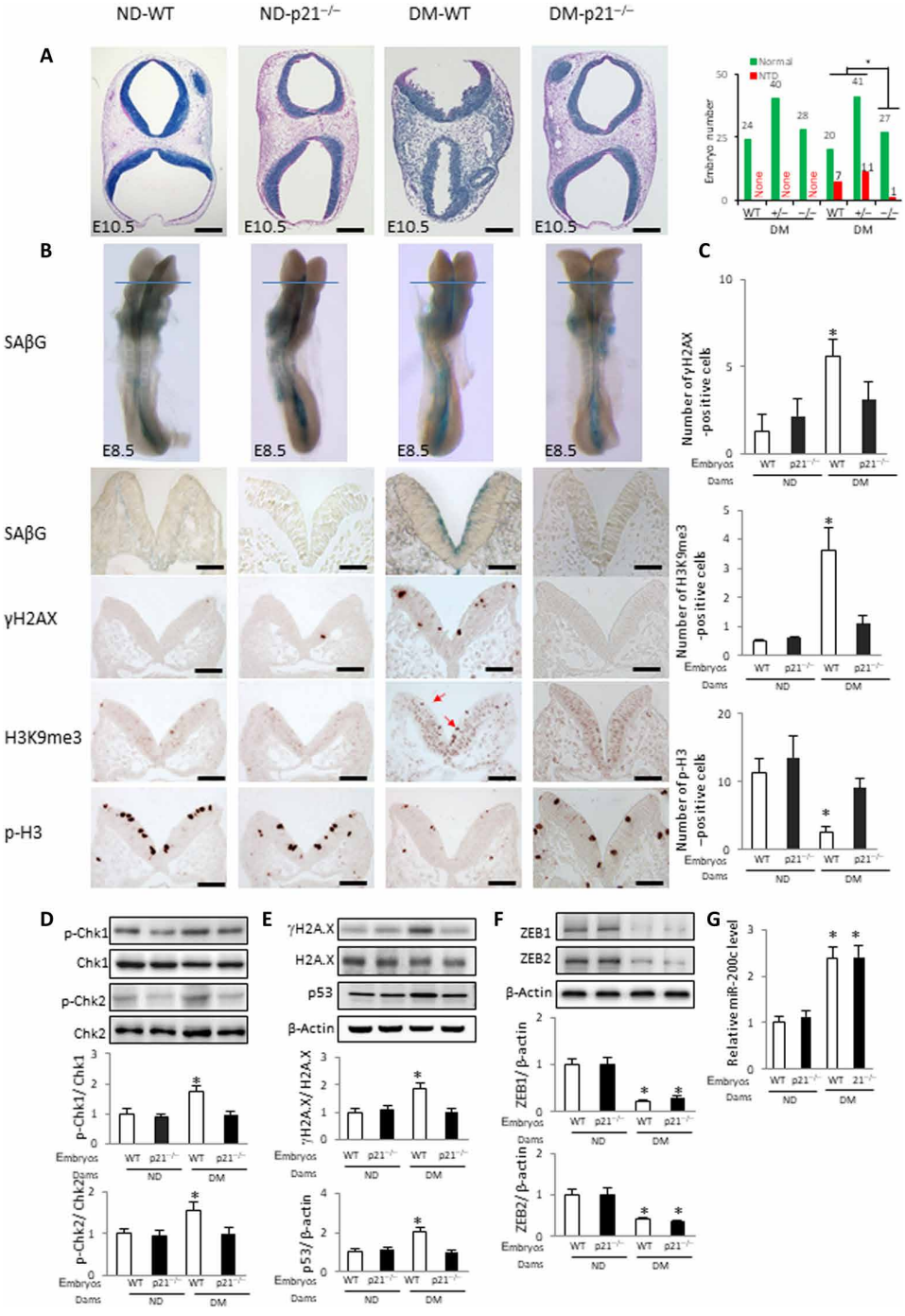

Fig. 5. Deletion of the senescence mediator p21 abrogates premature senescence. (**A**) Hematoxylin-eosin (HE) staining of E10.5 embryonic sections to show the open neural tube in NTD embryos and NTD rates of WT, p21-null, and heterozygous embryos is shown. Green bars, normal embryos; red bars, NTD embryos. (**B**) SAβG staining and antibody staining for γH2AX, H3K9me3 (red arrows), and p-H3. Quantification of antibody staining–positive cells is shown in (**C**). Protein abundance of phosphorylated p-Chk1, Chk1, p-Chk2, and Chk2 (**D**); γH2AX, H2AX, and p53 (**E**); and ZEB1 and ZEB2 (**F**) in E8.5 (five to seven somites) embryos. Bar graphs for protein abundance are quantitative data from three independent experiments ($n = 3$). Embryos from three litters ($n = 3$) each group and two to three embryos from each litter were analyzed. (**G**) mRNA abundance of miR-200c in E8.5 embryos. Embryos from three litters ($n = 3$) each group and two to three embryos from each litter were analyzed. Scale bars, 200 μm in (A), 70 μm in (B). Asterisk indicates a significant difference ($P < 0.05$) compared to other groups.

the basis of these findings, inhibition of premature senescence could be a potential intervention for diabetic embryopathy. It has been shown that rapamycin can inhibit cell entry into senescence (*37*). We showed that rapamycin inhibited diabetes-induced premature senescence in the developing neuroepithelium and reduced the number of apoptotic neuroepithelial cells, suggesting that rapamycin acts as a senomorphic agent that inhibits the initiation of senescence. Rapamycin is a Food and Drug Administration–approved

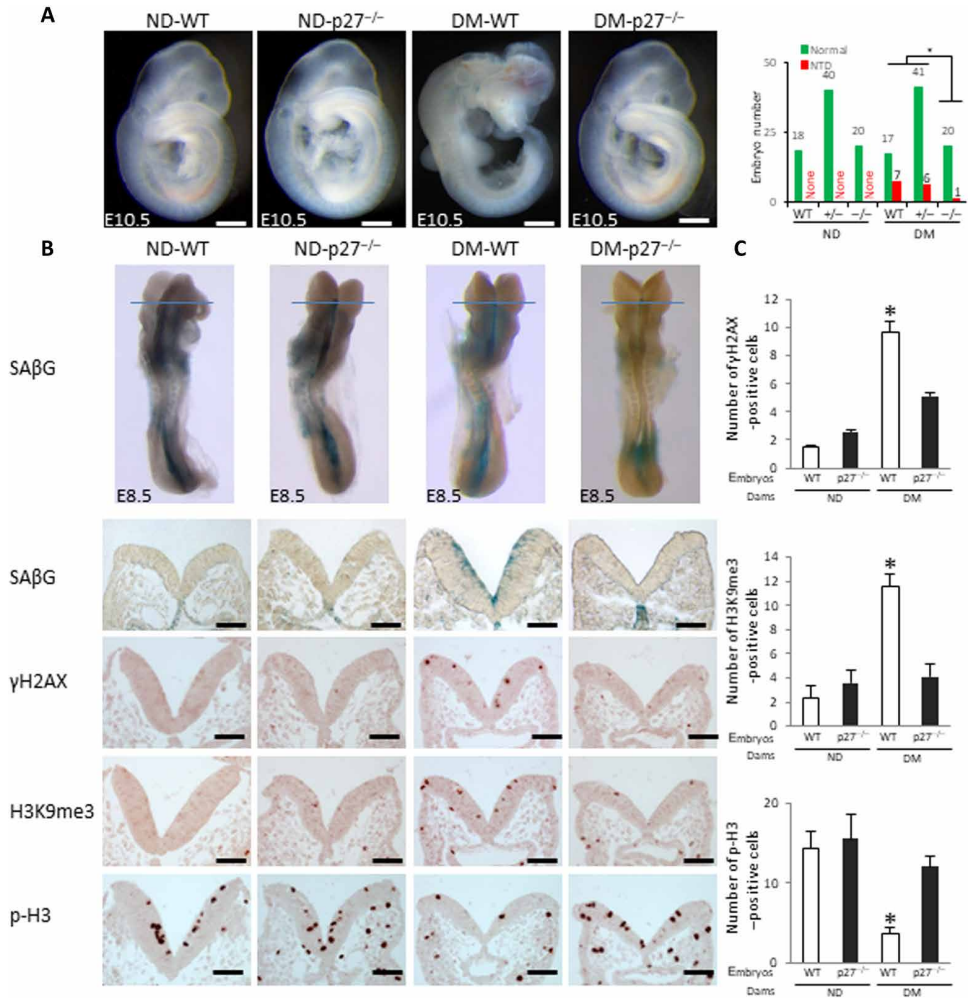

Fig. 6. Deletion of the senescence mediator p27 abrogates premature senescence. (**A**) HE staining of E10.5 embryonic sections and NTD rates of WT, p27-null, and heterozygous embryos is shown. Green bars, normal embryos; red bars, NTD embryos. (**B**) SAβG staining and antibody staining for γH2AX, H3K9me3, and p-H3. Quantification of antibody staining–positive cells is shown in (**C**). Scale bars, 200 μm in (A), 70 μm in (B). Embryos from three litters ($n = 3$) each group and two to three embryos from each litter were analyzed. Asterisk indicates a significant difference ($P < 0.05$) compared to other groups.

drug that prevents immune rejection of transplanted organs and has a good safety profile (*39*), and thus, it may be repurposed to treat diabetes-induced embryonic malformations as a senomorphic.

The degree of senescence in the neuroepithelium ranges from modest to severe. Modest senescence may not have any NTD manifestation and may result in other developmental defects, such as microcephaly (*9*), autism, and other developmental disabilities (*40*). Severe senescence results in NTD formation. In addition to neuroepithelial cell senescence, the occurrence of senescence in the cells comprising the tips of the two dorsal neural folds during the late phase of neurulation may also be required for NTD formation. Embryos with senescent cells in the dorsal neural fold tip fail to properly bend the dorsolateral hinge points and display wider gaps between the two neural fold tips than embryos without senescent cells in this area.

The current study provides genetic evidence supporting that the FoxO3a–miR-200c–ZEB1/2–p21/p27 pathway has a causal role in maternal diabetes–induced neuroepithelial cell premature senescence and NTD formation. Deletion of the *Foxo3a* gene, the *miR-200c* gene, the *p21* gene, or the *p27* gene abrogated senescence and ameliorated NTDs in embryos of diabetic dams. *p21* and *p27* transgenic (Tg) overexpression–induced neuroepithelial cell premature senescence and NTDs mimicked those observed in maternal diabetes. These findings collectively support our hypothesis that premature senescence in the neuroepithelium causes NTDs in diabetic pregnancies.

FoxO transcription factors regulate various cellular functions, including cell proliferation, apoptosis, aging, and oxidative stress. In adult cells, FoxO family members differentially regulate senescence. As a tumor suppressor, FoxO4 induces p21-dependent senescence in cancer cells (*41*). In contrast, FoxO3a suppresses senescence in aging cells (*42*). Therefore, FoxO factors regulate senescence in a cell type– and cellular context–dependent manner. Recent evidence supports the hypothesis that FoxO factors are senescence inducers during embryonic development (*12*). During normal embryogenesis, FoxO1 is the main stimulator of developmental senescence (*12*). In diabetic embryopathy, previous studies have demonstrated that maternal diabetes activates FoxO3a but not FoxO1 or FoxO4 (*8*).

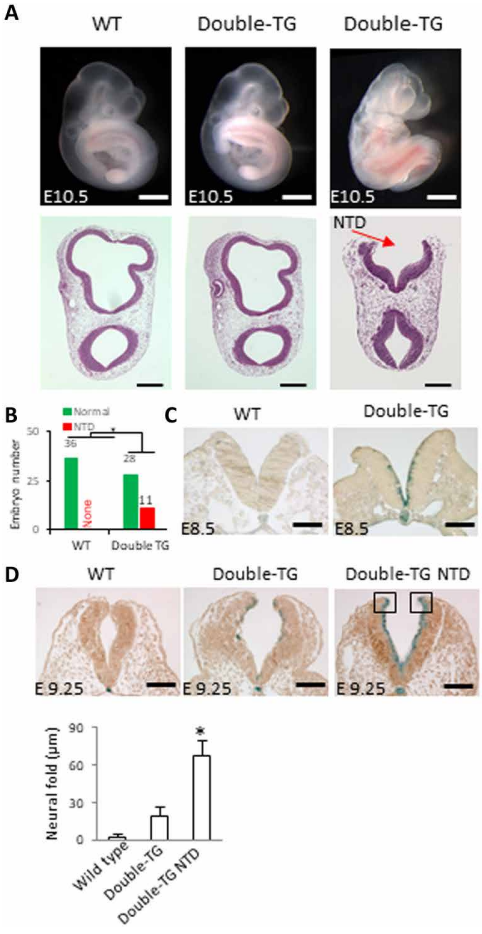

Fig. 7. The senescence mediators p21 and p27 mediate the teratogenicity of maternal diabetes, leading to NTD formation. (**A**) E10.5 whole embryos and HE staining sections of WT and p21/p27 double Tg embryos and (**B**) NTD rates in each group. Green bars, normal embryos; red bars, NTD embryos. (**C**) Coronal sections of E8.5 (five to seven somites) WT and p21/p27 double Tg embryos after SAβG staining. (**D**) Sections of E9.25 embryos after SAβG staining and quantification of the distance between the two neural fold fusion edges (square frames). Scale bars, 70 μm in (C) and (D) and 200 μm in (A). Embryos from three litters ($n = 3$) each group and two to three embryos from each litter were analyzed. Asterisk indicates a significant difference ($P < 0.05$) compared to other groups.

Both *Foxo3a* deletion and Tg overexpression of DN-FoxO3a blocked maternal diabetes–induced neuroepithelial senescence and NTD formation, strongly supporting FoxO3a as a senescence inducer in diabetic embryopathy.

FoxO factors could directly induce senescence through their transcriptional activity by inducing cell cycle inhibitors (*41*). However, the present study reveals that FoxO3a triggers neuroepithelial cell senescence by up-regulating miR-200c. Recent evidence implies that FoxO factors differentially regulate miRNA expression (*43*). We observed that deleting Foxo3a or overexpressing DN-FoxO3a in the neuroepithelium abolished the induction of miR-200c, supporting the concept that FoxO3a transcriptionally up-regulates miR-200c. miR-200c belongs to the miR-200 family, which consists of five members, including miR-141 and miR-200b. Both miR-200c and miR-141 can induce cellular senescence in vitro (*30*, *31*). miR-141 overexpression does not affect the preventive effect of miR-200c deletion on diabetic embryopathy. Therefore, only miR-200c appears to be involved in maternal diabetes–induced premature senescence in the developing neuroepithelium. This differential effect of miR-141 and miR-200c may be explained by their different seed sequences. miR-141 induces senescence by repressing the polycomb gene *BMI1*, leading to an increase in the cell cycle inhibitor p16 (*30*). In contrast, miR-200c silences ZEB1 and ZEB2, reversing the repression of p21 and p27, leading to premature senescence in the developing neuroepithelium.

p21 and p27 cooperatively induce senescence in the developing neuroepithelium. Individual deletion of either the *p21* gene or the *p27* gene abrogates premature senescence in diabetic embryopathy. p21 mediates not only developmental senescence but also the cellular senescence induced by a variety of stresses (*44*). In agreement with the present finding that *p21* gene deletion blocks the induction of premature senescence in diabetic embryopathy, ablation of p21 prevents both developmental senescence in vivo and stress-induced senescence in vitro (*12*, *45*). p27 is the closest cell cycle inhibitor to p21, and they belong to the same family of cell cycle inhibitors (*46*). Studies have also demonstrated that p27 contributes to senescent phenotypes (*47*). Furthermore, p27 directly induces senescence in adult cells (*48*, *49*). This evidence collectively supports the importance of both p21 and p27 in the induction of premature senescence in diabetic embryopathy. Both the p21 KO and p27 KO mouse models are ideal for the present study because deletion of either the *p21* gene or the *p27* gene does not affect neurulation and overall embryonic development (*50*, *51*). Although p27 KO female mice have reproductive problems (*51*), the study has circumvented these problems by effectively using the heterozygous mating scheme. The most notable finding from this study is that dual overexpression of p21 and p27 mimics maternal diabetes in inducing senescence in the neuroepithelium, leading to NTD formation.

Rapamycin is an mTOR inhibitor, whose activation leads to cell senescence (*52*). A previous study suggested that mTOR inhibition suppresses miR-200c expression and increases ZEB1/2 expression during epithelial-to-mesenchymal transition (*53*). Combined with the present results, mTOR and FoxO3a may cooperatively up-regulate miR-200c, leading to premature senescence in diabetic embryopathy. Furthermore, the mTOR effect may be mediated by its downstream effector, p70S6K1, whose activation critically participates in the induction of diabetic embryopathy (*54*). Rapamycin has been used in small clinical trials during pregnancy (*55*). However, the potential toxicity of rapamycin during pregnancy has not been carefully determined. Other senomorphics with confirmed safety profiling such as metformin may be a better choice than rapamycin (*56*).

In summary, the present study is the first to reveal a critical role for premature senescence in the neuroepithelium in diabetic embryopathy. The transcription factor FoxO3a, which is activated by oxidative stress (*8*), triggers a senescence pathway that involves miR-200c, ZEB1/2, p21, and p27. Proliferative metaphase neuroepithelial cells are primary targets of premature senescence in diabetic pregnancy, and senescence in these cells adversely affects the neurulation process by inhibiting neural fold bending and tip fusion. Thus, premature senescence is a new mechanism underlying failed neural tube closure in diabetic embryopathy. The senomorph-like agent rapamycin is an effective method to inhibit senescence and prevent diabetic embryopathy.

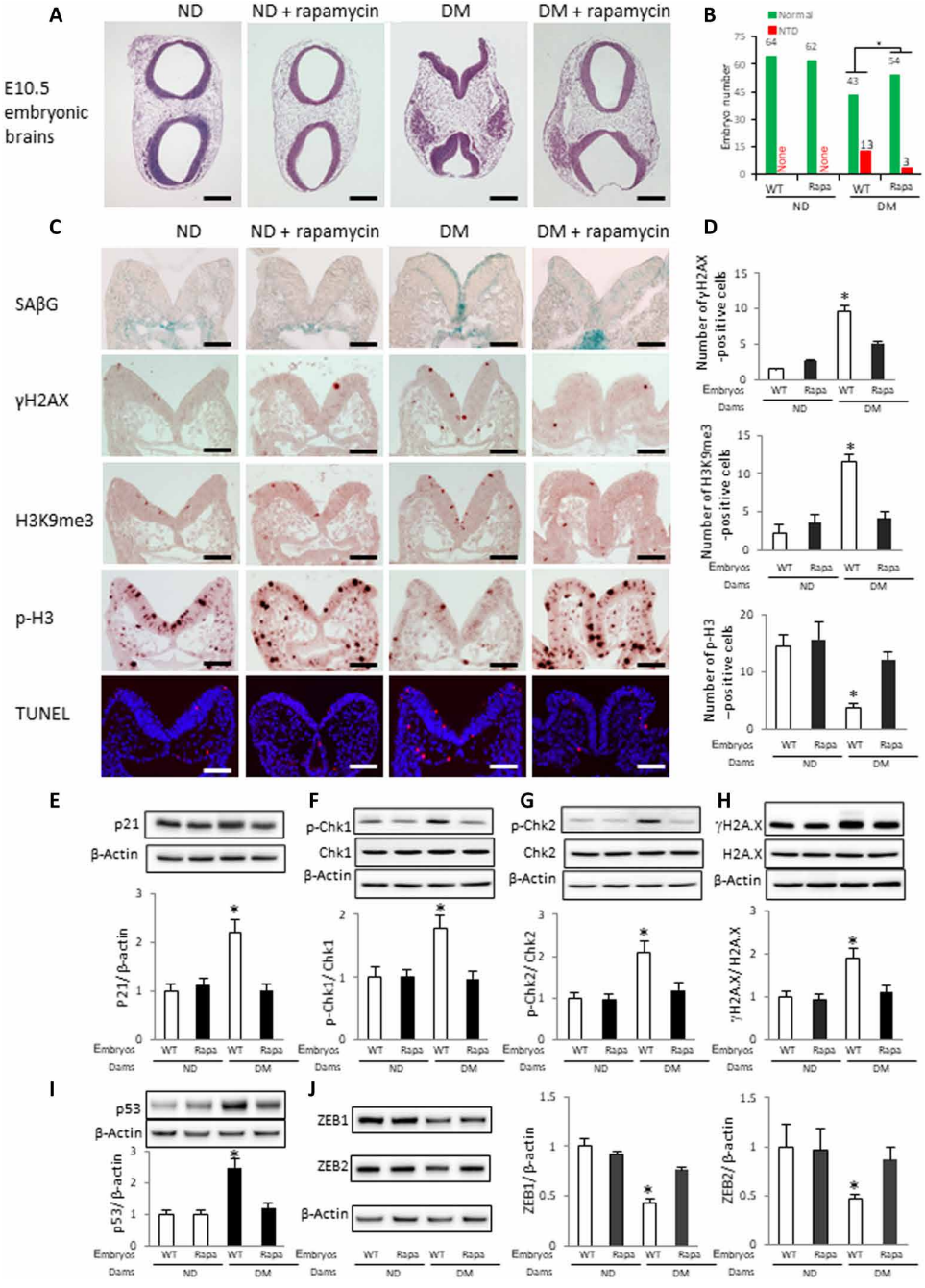

Fig. 8. Rapamycin inhibits premature senescence and reduces NTD formation. (**A**) HE staining of E10.5 embryonic sections from WT dams with or without rapamycin injection. (**B**) NTD rates in each group. Green bars, normal embryos; red bars, NTD embryos. (**C**) SAβG staining and antibody staining for γH2AX, H3K9me3, p-H3, and cell apoptosis detected by a TUNEL assay. Quantification of antibody staining is shown in (**D**). Protein abundances of p21 (**E**), p-Chk1 and total Chk1 (**F**), p-Chk2 and total Chk2 (**G**), γH2AX and total H2AX (**H**), p53 (**I**), and ZEB1 and ZEB2 (**J**) in E8.5 (five to seven somites) embryos. Bar graphs for protein abundance are quantitative data from three independent experiments ($n = 3$). Scale bars, 200 μm in (A) and 70 μm in (C). Embryos from three litters ($n = 3$) each group and two to three embryos from each litter were analyzed. Asterisk indicates a significant difference ($P < 0.05$) compared to other groups.

MATERIALS AND METHODS

Mice

All procedures for animal use were approved by the Institutional Animal Care and Use Committee of the University of Maryland School of Medicine. WT C57BL/6J mice and p21 KO, p27 KO, and FoxO3a KO mice were purchased from the Jackson laboratory (Bar Harbor, ME). The miR-200c/141 KO mouse with a C57BL/6J background was generated at Keio University School of Medicine (fig. S4) with a similar strategy for the miR-200b/429 KO mice (*57*). Male $p21^{+/-}$ or $p27^{+/-}$ heterozygous deletion mice were mated with non-diabetic or diabetic female $p21^{+/-}$ or $p27^{+/-}$ mice to generate WT, $p21^{+/-}$ or $p27^{+/-}$, and $p21^{-/-}$ or $p27^{-/-}$ embryos. Male $FoxO3a^{+/-}$ mice

were mated with nondiabetic or diabetic female FoxO3a$^{+/-}$ mice to generate WT, FoxO3a$^{+/-}$, and FoxO3a$^{-/-}$ embryos. Male miR-200c/141$^{+/-}$ mice were mated with nondiabetic or diabetic female miR-200c/141$^{+/-}$ mice to generate WT, miR-200c/141$^{+/-}$, and miR-200c/141$^{-/-}$ embryos.

Generation of DN-FoxO3a, miR-200c, miR-141, p21, and p27 Tg mice

DN-FoxO3a, miR-200c, miR-141, p21, and p27 Tg mice were generated by pronuclear injections using standard procedures at the Genome Modification Facility, Harvard University. The coding region of DN-FoxO3a was cloned from Addgene plasmid #1797 (*58*), a gift from M. Greenberg. Full-length mouse complementary DNA (cDNA) encoding pre-miR-200c, pre-miR-141, p21, and p27 with green fluorescent protein separately expressed was subcloned downstream of the rat nestin promoter, followed by a 3′ nestin genomic sequence. The Tg constructs were linearized to remove vector sequences, injected into fertilized oocytes from C57BL/6 female mice, and implanted into pseudopregnant mice. Three to four founders of each Tg line were generated, and founders with two- to fourfold transgene expression were selected for the experiments.

Model of diabetic embryopathy

We (*3*, *4*, *7*, *8*) and others (*59*) have used a rodent model of streptozotocin (STZ)–induced diabetes in research on diabetic embryopathy. Briefly, 10-week-old WT or KO female mice were intravenously injected daily with STZ (75 mg/kg) for 2 days to induce diabetes. STZ from Sigma-Aldrich (St. Louis, MO) was dissolved in sterile 0.1 M citrate buffer (pH 4.5). We used a U-100 insulin syringe (Becton Dickinson) with 28G1/2 needles for the injections. Approximately 140 μl of STZ solution was injected per mouse. Diabetes was defined as a 12-hour fasting blood glucose level of ≥16.7 mM. Male and female mice were paired at 3:00 p.m., and E0.5 of pregnancy was established at noon of the day when a vaginal plug was present. Embryos were harvested for subsequent analysis at different developmental stages. Embryos were harvested at 2:00 p.m. at E8.5 for biochemical and molecular analyses. At E10.5, embryos were examined under a Leica MZ16F stereomicroscope (Bannockburn, IL) for NTDs. Images of embryos were captured by a DFC420 5 MPix digital camera with software (Leica, Bannockburn, IL) and processed with Adobe Photoshop CS2. Normal embryos were classified as having a completely closed neural tube with no evidence of other malformations. Malformed embryos were classified as showing evidence of failed closure of the anterior neural tubes resulting in exencephaly, a lethal type of NTD with the absence of a major portion of the brain, skull, and scalp. Because our model induces NTD at E10.5, we did not examine other major structural malformations, such as cardiovascular defects, which do not occur until later embryonic stages (E13.5).

Rapamycin treatment administered to pregnant mice

Rapamycin (Selleck Chemicals, Houston, TX, USA) was dissolved in dimethyl sulfoxide to a concentration of 25 mg/ml and stored at −20°C. This stock solution was diluted by 50× to a concentration of 0.5 mg/ml with vehicle containing 5% Tween 80 and 30% polyethylene glycol, molecular weight 400. Pregnant WT diabetic and nondiabetic mice received intraperitoneal injections of rapamycin at a dose of 0.1 ml/g of body weight (2 mg/kg of body weight). Pregnant mice in the control groups (diabetic and nondiabetic) received the same volume of the vehicle solution. Rapamycin injections were given daily from E5.5 to E8.5 for biochemical and molecular analyses and to E10.5 for morphological examination.

Whole-mount senescence staining

For whole-mount embryo staining, embryos were fixed overnight in 0.5% glutaraldehyde prepared in phosphate-buffered saline (PBS) (pH 7.4). Embryos were washed with PBS/$MgCl_2$ (pH 5.5; 1 mM $MgCl_2$) for 2 × 15 min at 4°C on a rocker and then stained with X-gal staining solution containing 0.25 ml of X-gal stock (Roche, #745740) in *N*,*N*-dimethylformamide (Sigma-Aldrich, #D-4254), 0.25 ml of 0.2 M $K_3Fe(CN)_6$, 0.25 ml of 0.2 M $K_4Fe(CN)_6{\cdot}3H_2O$, and 9.25 ml of PBS/$MgCl_2$ for 4 hours. For embryo sectioning after senescence staining, embryos were embedded in optimal cutting temperature compound, sectioned (10 μm), and mounted on Superfrost slides for microscopy analysis.

Neuroepithelial cell isolation and flow cytometry analysis of senescent cells

E8.5 embryos were dissected out of the uterus, and then yolk sacs were removed from the embryos. Whole embryos were digested by Dispase II [3 mg/ml in PBS (pH 7.4)] for 15 min at room temperature to remove non-neural tissues. After enzymatic digestion, whole neuroepithelia were washed with PBS three times, cut into pieces, and digested with 0.25% trypsin-EDTA (Thermo Fisher Scientific) for 5 min at 37°C with shaking. The cell suspensions were centrifuged at 500*g* for 5 min and resuspended in Dulbecco's modified Eagle's medium (DMEM; Thermo Fisher Scientific) with 10% fetal bovine serum (FBS; Thermo Fisher Scientific) followed by filtration through a 70-μm cell strainer. The isolated cells were seeded in six-well plates.

Live cell senescence analysis was performed using the Cellular Senescence Live Cell Analysis Assay Kit (Enzo Life Sciences). Briefly, after adhesion, the isolated neuroepithelial cells were treated with 2 ml of 1× cell pretreatment solution for 2 hours at 37°C. Then, 10 μl of 200× SAβG substrate solution was directly added to 1× cell pretreatment solution, gently mixed, and incubated at 37°C for 4 hours. After senescence staining, the cells were washed with PBS three times. The stained cells were fixed and permeabilized by Fixation and Permeabilization solution (BD Biosciences) followed by immunostaining using an anti-p21 antibody (table S10) and a fluorescence-coupled secondary antibody. Last, the cells were washed and analyzed by a flow cytometer.

Immunostaining and hematoxylin-eosin staining

Embryos at various stages were fixed in methacarn (60% methanol, 30% chloroform, and 10% glacial acetic acid), embedded in paraffin, and cut into 5-μm sections. After deparaffinization and rehydration, all specimens were subjected to immunofluorescence staining for p21 and p27 and immunohistochemical staining for γH2AX, H3K9me3, p-H3, and F4/80 using the respective antibodies (table S10) or hematoxylin-eosin staining. All sections were photographed.

Cell culture and miR-200c mimic and inhibitor transfection

C17.2 mouse neural stem cells, originally obtained from the European Collection of Cell Culture, were maintained in DMEM (5 mM glucose) supplemented with 10% FBS, penicillin (100 U/ml), and streptomycin (100 μg/ml) at 37°C in a humidified atmosphere of 5% CO_2. Although C17.2 cells are newborn mouse cerebellar progenitor cells transformed

with retroviral v-myc, these cells mimic in vivo neuroepithelial cells in response to high glucose (*60*). Lipofectamine RNAiMAX (Invitrogen) was used according to the manufacturer's protocol for transfection of the miR-200c mimic and inhibitor into the cells under 1% FBS culture conditions. The mirVana miR mimic and the miR inhibitor of miR-200c were purchased from Ambion.

MiR-200 promoter activity analysis

The binding sites of the transcription factor FoxO3a, which potentially regulates miR-200 promoter activity, were predicted using online prediction tools (http://jaspar.genereg.net). We identified two FoxO3a binding sites in the miR-200 promoter region. The miR-200 promoter was subcloned and inserted into a pGL4.10 Luciferase Reporter Vector (Promega). Cotransfection of FoxO3a constitutively active (CA-FoxO3a) or dominant-negative (DN-FoxO3a) vector and the pGL4.1-miR200 promoter vector into the mouse neural stem cell line C17.2 was performed using Lipofectamine 2000 (Invitrogen), and the cells were cultured for 48 hours with or without treatment with high glucose (25 mM). The CA-FoxO3a vector (Addgene plasmid #1788) and DN-FoxO3a vector (Addgene plasmid #1797) were gifts from M. Greenberg, at the Department of Neurobiology, Harvard Medical School (*58*). Cells were harvested and lysed using lysis buffer from the Dual-Luciferase Assay System (Promega). Firefly luciferase activities were normalized to that of the internal control *Renilla* luciferase.

Immunoblotting

Equal amounts of protein from embryos were resolved by SDS–polyacrylamide gel electrophoresis and transferred onto Immobilon-P membranes (Millipore). Membranes were incubated in 5% nonfat milk for 45 min at room temperature and then incubated for 18 hours at 4°C with primary antibodies against the following molecules diluted in 5% nonfat milk: p21, p27, phospho-Chk1, Chk1, phospho-Chk2, Chk2, ZEB1, ZEB2, p53, and γH2AX (table S10). Membranes were then exposed to goat anti-rabbit or anti-mouse secondary antibodies. To confirm that equivalent amounts of protein were loaded among samples, membranes were stripped and probed with a mouse antibody against β-actin (table S10). Signals were detected using a SuperSignal West Femto Maximum Sensitivity Substrate Kit (Thermo Fisher Scientific). All experiments were repeated three times with the use of independently prepared tissue lysates.

Quantitative reverse transcription polymerase chain reaction

Total RNA was isolated from tissues and cells using TRIzol reagent (Ambion) and reverse-transcribed using the QuantiTect Reverse Transcription Kit (Qiagen). Reverse transcription for miRNA was performed using the qScript microRNA cDNA Synthesis Kit (Quanta Biosciences). Quantitative reverse transcription polymerase chain reaction (RT-qPCR) of mRNA, pri-miRNA, and small nuclear RNA U6 was performed using the Maxima SYBR Green/ROX qPCR Master Mix assay (Thermo Fisher Scientific). The primers for RT-qPCR are listed in table S11. RT-qPCR and subsequent calculations were performed by a StepOnePlus Real-Time PCR System (Applied Biosystem).

miRNA pull-down

The biotin-labeled miR-200c and its control (*Caenorhabditis elegans* miR-67) were custom-made by GE Dharmacon. The biotin-labeled miR-200c and biotin-labeled negative control were transfected using Lipofectamine 2000 (Invitrogen) into C17.2 cells for 48 hours, and then cells were lysed in lysis buffer [20 mM tris-HCl (pH 7.5), 100 mM KCl, 5 mM $MgCl_2$, and 0.3% IGEPAL CA-630]. Cell lysates were mixed with streptavidin-coupled Dynabeads (Invitrogen) and incubated at 4°C on a rotator overnight. After the beads were washed thoroughly, the bead-bound RNA was isolated and subjected to RT followed by real-time PCR analysis.

Statistical analyses

All experiments were completely randomized and repeated in triplicate. Specifically, embryos from three litters each group were analyzed as we previously described (*8*–*10*). For immunostaining, two to three embryos from each litter and four to five sections per embryo were stained, and an average for signal intensity was obtained for that litter. For immunoblotting, two to three embryos from a litter in each group were combined for a single run, and there were three runs per experiment. For RT-qPCR, two to three embryos per litter were combined, and three litters per group were analyzed. For cell culture studies, experiments were repeated in triplicate as we previously described (*60*). Data are presented as the means ± SEs. Student's *t* test was used for two group comparisons. One-way analysis of variance (ANOVA) was performed for comparisons of more than two groups using SigmaStat 3.5 software. In ANOVA, a Tukey test was used to estimate the significance. Significant differences between groups in NTD incidence expressed by the number of embryos were analyzed by the chi-square test or Fisher's exact test using SigmaStat 3.5 software. Differences were considered statistically significant when $P < 0.05$.

SUPPLEMENTARY MATERIALS

Supplementary material for this article is available at http://advances.sciencemag.org/cgi/content/full/7/27/eabf5089/DC1

View/request a protocol for this paper from *Bio-protocol*.

REFERENCES AND NOTES

1. P. Cavalli, Prevention of neural tube defects and proper folate periconceptional supplementation. *J. Prenat. Med.* **2**, 40–41 (2008).
2. A. Correa, S. M. Gilboa, L. M. Besser, L. D. Botto, C. A. Moore, C. A. Hobbs, M. A. Cleves, T. J. Riehle-Colarusso, D. K. Waller, E. A. Reece, Diabetes mellitus and birth defects. *Am. J. Obstet. Gynecol.* **199**, 237.e1–237.e9 (2008).
3. X. Li, H. Weng, C. Xu, E. A. Reece, P. Yang, Oxidative stress–induced JNK1/2 activation triggers proapoptotic signaling and apoptosis that leads to diabetic embryopathy. *Diabetes* **61**, 2084–2092 (2012).
4. X. Li, C. Xu, P. Yang, c-Jun NH_2-Terminal Kinase 1/2 and endoplasmic reticulum stress as interdependent and reciprocal causation in diabetic embryopathy. *Diabetes* **62**, 599–608 (2013).
5. Y. Wu, F. Wang, M. Fu, C. Wang, M. J. Quon, P. Yang, Cellular stress, excessive apoptosis, and the effect of metformin in a mouse model of type 2 diabetic embryopathy. *Diabetes* **64**, 2526–2536 (2015).
6. P. Yang, Z. Zhao, E. A. Reece, Activation of oxidative stress signaling that is implicated in apoptosis with a mouse model of diabetic embryopathy. *Am. J. Obstet. Gynecol.* **198**, 130.e1–137.e7 (2008).
7. H. Gu, J. Yu, D. Dong, Q. Zhou, J.-Y. Wang, S. Fang, P. Yang, High glucose–repressed CITED2 expression through miR-200b triggers the unfolded protein response and endoplasmic reticulum stress. *Diabetes* **65**, 149–163 (2016).
8. P. Yang, X. Li, C. Xu, R. L. Eckert, E. A. Reece, H. R. Zielke, F. Wang, Maternal hyperglycemia activates an ASK1-FoxO3a-Caspase 8 pathway that leads to embryonic neural tube defects. *Sci. Signal.* **6**, ra74 (2013).
9. F. Wang, C. Xu, E. A. Reece, X. Li, Y. Wu, C. Harman, J. Yu, D. Dong, C. Wang, P. Yang, J. Zhong, P. Yang, Protein kinase C-alpha suppresses autophagy and induces neural tube defects via miR-129-2 in diabetic pregnancy. *Nat. Commun.* **8**, 15182 (2017).
10. P. Yang, C. Xu, E. A. Reece, X. Chen, J. Zhong, M. Zhan, D. J. Stumpo, P. J. Blackshear, P. Yang, Tip60- and sirtuin 2-regulated MARCKS acetylation and phosphorylation are required for diabetic embryopathy. *Nat. Commun.* **10**, 282 (2019).

11. M. Storer, A. Mas, A. Robert-Moreno, M. Pecoraro, M. C. Ortells, V. di Giacomo, R. Yosef, N. Pilpel, V. Krizhanovsky, J. Sharpe, W. M. Keyes, Senescence is a developmental mechanism that contributes to embryonic growth and patterning. *Cell* **155**, 1119–1130 (2013).
12. D. Muñoz-Espín, M. Cañamero, A. Maraver, G. Gómez-López, J. Contreras, S. Murillo-Cuesta, A. Rodríguez-Baeza, I. Varela-Nieto, J. Ruberte, M. Collado, M. Serrano, Programmed cell senescence during mammalian embryonic development. *Cell* **155**, 1104–1118 (2013).
13. T. Kuilman, C. Michaloglou, L. C. W. Vredeveld, S. Douma, R. van Doorn, C. J. Desmet, L. A. Aarden, W. J. Mooi, D. S. Peeper, Oncogene-induced senescence relayed by an interleukin-dependent inflammatory network. *Cell* **133**, 1019–1031 (2008).
14. A. T. Lee, D. Reis, U. J. Eriksson, Hyperglycemia-induced embryonic dysmorphogenesis correlates with genomic DNA mutation frequency in vitro and in vivo. *Diabetes* **48**, 371–376 (1999).
15. L. Pani, M. Horal, M. R. Loeken, Polymorphic susceptibility to the molecular causes of neural tube defects during diabetic embryopathy. *Diabetes* **51**, 2871–2874 (2002).
16. T. Yokoi, K. Fukuo, O. Yasuda, M. Hotta, J. Miyazaki, Y. Takemura, H. Kawamoto, H. Ichijo, T. Ogihara, Apoptosis signal-regulating kinase 1 mediates cellular senescence induced by high glucose in endothelial cells. *Diabetes* **55**, 1660–1665 (2006).
17. S. Macip, M. Igarashi, L. Fang, A. Chen, Z.-Q. Pan, S. W. Lee, S. A. Aaronson, Inhibition of p21-mediated ROS accumulation can rescue p21-induced senescence. *EMBO J.* **21**, 2180–2188 (2002).
18. S. G. McShane, M. A. Molè, D. Savery, N. D. E. Greene, P. P. L. Tam, A. J. Copp, Cellular basis of neuroepithelial bending during mouse spinal neural tube closure. *Dev. Biol.* **404**, 113–124 (2015).
19. E. Nikolopoulou, G. L. Galea, A. Rolo, N. D. Greene, A. J. Copp, Neural tube closure: Cellular, molecular and biomechanical mechanisms. *Development* **144**, 552–566 (2017).
20. E.-C. Kim, J.-R. Kim, Senotherapeutics: Emerging strategy for healthy aging and age-related disease. *BMB Rep.* **52**, 47–55 (2019).
21. T. Tchkonia, Y. Zhu, J. van Deursen, J. Campisi, J. L. Kirkland, Cellular senescence and the senescent secretory phenotype: Therapeutic opportunities. *J. Clin. Invest.* **123**, 966–972 (2013).
22. F. C. Sauer, Mitosis in the neural tube. *J. Comp. Neurol.* **62**, 377–405 (1935).
23. J. Langman, R. L. Guerrant, B. G. Freeman, Behavior of neuro-epithelial cells during closure of the neural tube. *J. Comp. Neurol.* **127**, 399–411 (1966).
24. C. Skurk, H. Maatz, H.-S. Kim, J. Yang, M. R. Abid, W. C. Aird, K. Walsh, The Akt-regulated forkhead transcription factor FOXO3a controls endothelial cell viability through modulation of the caspase-8 inhibitor FLIP. *J. Biol. Chem.* **279**, 1513–1525 (2004).
25. D. P. Bartel, MicroRNAs: Target recognition and regulatory functions. *Cell* **136**, 215–233 (2009).
26. A. R. Colas, W. L. McKeithan, T. J. Cunningham, P. J. Bushway, L. X. Garmire, G. Duester, S. Subramaniam, M. Mercola, Whole-genome microRNA screening identifies *let-7* and *mir-18* as regulators of germ layer formation during early embryogenesis. *Genes Dev.* **26**, 2567–2579 (2012).
27. P. Mukhopadhyay, G. Brock, S. Appana, C. Webb, R. M. Greene, M. M. Pisano, MicroRNA gene expression signatures in the developing neural tube. *Birth Defects Res. A Clin. Mol. Teratol.* **91**, 744–762 (2011).
28. H. Gu, H. Li, L. Zhang, H. Luan, T. Huang, L. Wang, Y. Fan, Y. Zhang, X. Liu, W. Wang, Z. Yuan, Diagnostic role of microRNA expression profile in the serum of pregnant women with fetuses with neural tube defects. *J. Neurochem.* **122**, 641–649 (2012).
29. H. Gu, J. Yu, D. Dong, Q. Zhou, J. Y. Wang, P. Yang, The miR-322-TRAF3 circuit mediates the pro-apoptotic effect of high glucose on neural stem cells. *Toxicol. Sci.* **144**, 186–196 (2015).
30. M. Dimri, J. D. Carroll, J.-H. Cho, G. P. Dimri, microRNA-141 regulates BMI1 expression and induces senescence in human diploid fibroblasts. *Cell Cycle* **12**, 3537–3546 (2013).
31. A. Magenta, C. Cencioni, P. Fasanaro, G. Zaccagnini, S. Greco, G. Sarra-Ferraris, A. Antonini, F. Martelli, M. C. Capogrossi, miR-200c is upregulated by oxidative stress and induces endothelial cell apoptosis and senescence via ZEB1 inhibition. *Cell Death Differ.* **18**, 1628–1639 (2011).
32. Y. Itahana, S. H. Neo, K. Itahana, miR-141, a new player, joins the senescence orchestra. *Cell Cycle* **12**, 3586–3587 (2013).
33. P. A. Gregory, A. G. Bert, E. L. Paterson, S. C. Barry, A. Tsykin, G. Farshid, M. A. Vadas, Y. Khew-Goodall, G. J. Goodall, The miR-200 family and miR-205 regulate epithelial to mesenchymal transition by targeting ZEB1 and SIP1. *Nat. Cell Biol.* **10**, 593–601 (2008).
34. Y. Liu, S. El-Naggar, D. S. Darling, Y. Higashi, D. C. Dean, Zeb1 links epithelial-mesenchymal transition and cellular senescence. *Development* **135**, 579–588 (2008).
35. Y. Liu, E. Sánchez-Tilló, X. Lu, L. Huang, B. Clem, S. Telang, A. B. Jenson, M. Cuatrecasas, J. Chesney, A. Postigo, D. C. Dean, Sequential inductions of the ZEB1 transcription factor caused by mutation of Rb and then Ras proteins are required for tumor initiation and progression. *J. Biol. Chem.* **288**, 11572–11580 (2013).
36. S. Qi, Y. Song, Y. Peng, H. Wang, H. Long, X. Yu, Z. Li, L. Fang, A. Wu, W. Luo, Y. Zhen, Y. Zhou, Y. Chen, C. Mai, Z. Liu, W. Fang, ZEB2 mediates multiple pathways regulating cell proliferation, migration, invasion, and apoptosis in glioma. *PLOS ONE* **7**, e38842 (2012).
37. A. M. Nicaise, L. J. Wagstaff, C. M. Willis, C. Paisie, H. Chandok, P. Robson, V. Fossati, A. Williams, S. J. Crocker, Cellular senescence in progenitor cells contributes to diminished remyelination potential in progressive multiple sclerosis. *Proc. Natl. Acad. Sci. U.S.A.* **116**, 9030–9039 (2019).
38. L. J. Hickson, L. G. P. Langhi Prata, S. A. Bobart, T. K. Evans, N. Giorgadze, S. K. Hashmi, S. M. Herrmann, M. D. Jensen, Q. Jia, K. L. Jordan, T. A. Kellogg, S. Khosla, D. M. Koerber, A. B. Lagnado, D. K. Lawson, N. K. LeBrasseur, L. O. Lerman, K. M. McDonald, T. J. McKenzie, J. F. Passos, R. J. Pignolo, T. Pirtskhalava, I. M. Saadiq, K. K. Schaefer, S. C. Textor, S. G. Victorelli, T. L. Volkman, A. Xue, M. A. Wentworth, E. O. Wissler Gerdes, Y. Zhu, T. Tchkonia, J. L. Kirkland, Senolytics decrease senescent cells in humans: Preliminary report from a clinical trial of dasatinib plus quercetin in individuals with diabetic kidney disease. *EBioMedicine* **47**, 446–456 (2019).
39. S. Bak, S. Tischer, A. Dragon, S. Ravens, L. Pape, C. Koenecke, M. Oelke, R. Blaszczyk, B. Maecker-Kolhoff, B. Eiz-Vesper, Selective effects of mTOR inhibitor sirolimus on naïve and CMV-specific T cells extending its applicable range beyond immunosuppression. *Front. Immunol.* **9**, 2953 (2018).
40. M. Li, M. D. Fallin, A. Riley, R. Landa, S. O. Walker, M. Silverstein, D. Caruso, C. Pearson, S. Kiang, J. L. Dahm, X. Hong, G. Wang, M.-C. Wang, B. Zuckerman, X. Wang, The association of maternal obesity and diabetes with autism and other developmental disabilities. *Pediatrics* **137**, e20152206 (2016).
41. P. L. J. de Keizer, L. M. Packer, A. A. Szypowska, P. E. Riedl-Polderman, N. J. F. van den Broek, A. de Bruin, T. B. Dansen, R. Marais, A. B. Brenkman, B. M. T. Burgering, Activation of forkhead box O transcription factors by oncogenic BRAF promotes $p21^{cip1}$-dependent senescence. *Cancer Res.* **70**, 8526–8536 (2010).
42. K. S. Kim, M.-S. Kim, Y. B. Seu, H. Y. Chung, J. H. Kim, J.-R. Kim, Regulation of replicative senescence by insulin-like growth factor-binding protein 3 in human umbilical vein endothelial cells. *Aging Cell* **6**, 535–545 (2007).
43. X. Liu, J. Feng, L. Tang, L. Liao, Q. Xu, S. Zhu, The regulation and function of miR-21-FOXO3a-miR-34b/c signaling in breast cancer. *Int. J. Mol. Sci.* **16**, 3148–3162 (2015).
44. T. Kuilman, C. Michaloglou, W. J. Mooi, D. S. Peeper, The essence of senescence. *Genes Dev.* **24**, 2463–2479 (2010).
45. V. Gire, P. Roux, D. Wynford-Thomas, J. M. Brondello, V. Dulic, DNA damage checkpoint kinase Chk2 triggers replicative senescence. *EMBO J.* **23**, 2554–2563 (2004).
46. C. J. Sherr, J. M. Roberts, CDK inhibitors: Positive and negative regulators of G_1-phase progression. *Genes Dev.* **13**, 1501–1512 (1999).
47. M. Collado, M. Serrano, The power and the promise of oncogene-induced senescence markers. *Nat. Rev. Cancer* **6**, 472–476 (2006).
48. P. K. Majumder, C. Grisanzio, F. O'Connell, M. Barry, J. M. Brito, Q. Xu, I. Guney, R. Berger, P. Herman, R. Bikoff, G. Fedele, W.-K. Baek, S. Wang, K. Ellwood-Yen, H. Wu, C. L. Sawyers, S. Signoretti, W. C. Hahn, M. Loda, W. R. Sellers, A prostatic intraepithelial neoplasia-dependent $p27^{Kip1}$ checkpoint induces senescence and inhibits cell proliferation and cancer progression. *Cancer Cell* **14**, 146–155 (2008).
49. J. M. Flores, J. Martín-Caballero, R. A. García-Fernández, p21 and p27 a shared senescence history. *Cell Cycle* **13**, 1655–1656 (2014).
50. C. Deng, P. Zhang, J. W. Harper, S. J. Elledge, P. Leder, Mice lacking $p21^{CIP1/WAF1}$ undergo normal development, but are defective in G1 checkpoint control. *Cell* **82**, 675–684 (1995).
51. Y. Geng, Q. Yu, E. Sicinska, M. Das, R. T. Bronson, P. Sicinski, Deletion of the $p27^{Kip1}$ gene restores normal development in cyclin D1-deficient mice. *Proc. Natl. Acad. Sci. U.S.A.* **98**, 194–199 (2001).
52. A. Houssaini, M. Breau, K. Kebe, S. Abid, E. Marcos, L. Lipskaia, D. Rideau, A. Parpaleix, J. Huang, V. Amsellem, N. Vienney, P. Validire, B. Maitre, A. Attwe, C. Lukas, D. Vindrieux, J. Boczkowski, G. Derumeaux, M. Pende, D. Bernard, S. Meiners, S. Adnot, mTOR pathway activation drives lung cell senescence and emphysema. *JCI Insight* **3**, e93203 (2018).
53. I. Mikaelian, M. Malek, R. Gadet, J. Viallet, A. Garcia, A. Girard-Gagnepain, C. Hesling, G. Gillet, P. Gonzalo, R. Rimokh, M. Billaud, Genetic and pharmacologic inhibition of mTORC1 promotes EMT by a TGF-β–independent mechanism. *Cancer Res.* **73**, 6621–6631 (2013).
54. S. Cao, W.-B. Shen, E. A. Reece, P. Yang, Deficiency of the oxidative stress-responsive kinase p70S6K1 restores autophagy and ameliorates neural tube defects in diabetic embryopathy. *Am. J. Obstet. Gynecol.* **223**, 753.e1–753.e14 (2020).
55. H. Park, C. S. Chang, S.-J. Choi, S.-y. Oh, C.-R. Roh, Sirolimus therapy for fetal cardiac rhabdomyoma in a pregnant woman with tuberous sclerosis. *Obstet. Gynecol. Sci.* **62**, 280–284 (2019).
56. Q. Hu, J. Peng, L. Jiang, W. Li, Q. Su, J. Zhang, H. Li, M. Song, B. Cheng, J. Xia, T. Wu, Metformin as a senostatic drug enhances the anticancer efficacy of CDK4/6 inhibitor in head and neck squamous cell carcinoma. *Cell Death Dis.* **11**, 925 (2020).
57. H. Hasuwa, J. Ueda, M. Ikawa, M. Okabe, miR-200b and miR-429 function in mouse ovulation and are essential for female fertility. *Science* **341**, 71–73 (2013).

58. H. Tran, A. Brunet, J. M. Grenier, S. R. Datta, A. J. Fornace Jr., P. S. Di Stefano, L. W. Chiang, M. E. Greenberg, DNA repair pathway stimulated by the forkhead transcription factor FOXO3a through the Gadd45 protein. *Science* **296**, 530–534 (2002).
59. J. M. Salbaum, C. Kappen, Neural tube defect genes and maternal diabetes during pregnancy. *Birth Defects Res. A Clin. Mol. Teratol.* **88**, 601–611 (2010).
60. F. Wang, Y. Wu, H. Gu, E. A. Reece, S. Fang, R. Gabbay-Benziv, G. Aberdeen, P. Yang, *Ask1* gene deletion blocks maternal diabetes–induced endoplasmic reticulum stress in the developing embryo by disrupting the unfolded protein response signalosome. *Diabetes* **64**, 973–988 (2015).

Acknowledgments: We appreciate the Genome Modification Facility, Harvard University, for generating FoxO3a-DN Tg, miR-141 Tg, miR-200c Tg, p21 Tg, and double p21/p27 Tg mice. We thank J. A. Rosen at the University of Maryland School of Medicine for critical review and editing assistance, X. Chen at the University of Maryland School of Medicine for assisting with the cell sorting analysis, and D. Dong at the University of Maryland School of Medicine for assisting with the miR-200c study. **Funding:** This work was supported by NIH grants NIH HD100195, R01HD102206, R01HD099843, R01DK083243, R01DK101972, R01HL131737, R01HL134368, R01HL139060, and R01DK103024. **Author contributions:** C.X. researched and organized the data. P.Y. conceived the project, designed the experiments, and wrote the manuscript. H.H. generated the miR-200C KO mice and reviewed the manuscript. E.A.R., C.H., S.K., and W.-B.S. analyzed and reviewed the manuscript. **Competing interests:** The authors declare that they have no competing interests. **Data and materials availability:** All data needed to evaluate the conclusions in the paper are present in the paper and/or the Supplementary Materials. Additional data related to this paper may be requested from the authors.

Submitted 30 October 2020
Accepted 18 May 2021
Published 30 June 2021
10.1126/sciadv.abf5089

Citation: C. Xu, W.-B. Shen, E. A. Reece, H. Hasuwa, C. Harman, S. Kaushal, P. Yang, Maternal diabetes induces senescence and neural tube defects sensitive to the senomorphic rapamycin. *Sci. Adv.* **7**, eabf5089 (2021).